Thermoelastic stress in GaAs/AlGaAs quantum cascade lasers

Vincenzo Spagnolo,[a] Gaetano Scamarcio,[b] and Danilo Marano
INFM, Dipartimento Interateneo di Fisica, Università e Politecnico di Bari via Amendola 173, 70126 Bari, Italy

Hideaki Page and Carlo Sirtori
Thales Research and Technology, Domaine de Corbeville, 91404 Orsay, France

(Received 4 February 2003; accepted 25 April 2003)

We have determined the shear stress associated with the temperature gradient in quantum cascade lasers operated in continuous-wave mode. This information was obtained as a function of the electrical power using a combination of microprobe photoluminescence and anti-Stokes/Stokes Raman measurements in ridge-waveguide GaAs structures mounted epilayer down to the heat sink. At electrical power densities in the order of ~ 5 kW/cm^2, the strain in the cladding layers at the edges of the laser ridges reaches the critical value for the creation of misfit dislocations. Above 10–12 kW/cm^2, extended defect formation and eventual device failure are observed. © *2003 American Institute of Physics.* [DOI: 10.1063/1.1586998]

Quantum cascade lasers (QCLs) are the most advanced class of semiconductor sources operating in the midinfrared spectral range of 3.5–16 μm.[1,2] The attainment of continuous-wave (cw) operation at room temperature, achieved using a buried waveguide, is a breakthrough confirming the potential of QCLs for applications such as trace-gas sensing and free-space optical communications.[3] Since high-temperature cw operation remains the only impediment to the wide industrial use of these lasers, progress in the thermal management and in the understanding of thermoelastic effects is needed.[3]

Two features determine the large electrical powers dissipated into the active region, typically two orders of magnitude higher than those of comparable diode lasers: (i) The high applied voltages (5–10 V) and (ii) the large threshold currents, typically several kA/cm^2, due to the high losses (10–30 cm^{-1}) of midinfrared laser cavities. Further, the heat dissipation in the active region is poor because of the low thermal conductivity of ternary-alloy semiconductors and the large number (500–1000) of interfaces. This produces stress fields related to active region temperatures much higher than the heat sink ones and large temperature gradients.[4,5] High values of strain may trigger the nucleation and propagation of misfit dislocations, voids, and cracks[6] and has been suggested as the main reason for QCL failure,[3] although no experimental evidence has been reported yet.

In this work, we have measured the thermally induced strain in GaAs cw-operated ridge-waveguide QCLs mounted epilayer down to the heat sink. We used a combination of microprobe anti-Stokes/Stokes (AS/S) Raman and photoluminescence (PL) spectroscopies. A GaAs/$Al_{0.45}Ga_{0.55}As$ laser structure was grown on a GaAs substrate. The active layer, consisting of 36 periods of a GaAs/$Al_{0.45}Ga_{0.55}As$ heterostructure (total thickness 1.63 μm) designed for emission at 9.0 μm, is sandwiched between two 4.5 μm thick GaAs cladding layers. Ridge waveguides (2 mm long and 30 μm wide) were defined using photolithographic techniques, wet etching 10 μm deep trenches through the active region. Instead of dielectric layers, ion implantation was used to electrically isolate the regions bordering the laser ridges. The strong refractive index contrast at the walls of the laser ridge and the absence of dielectric materials allow effective mode confinement in the lateral direction as well as low losses. Two similar devices were mounted epilayer down on copper–tungsten (CuW) heat sinks and then soldered onto copper mounts. The devices were mounted on the cold finger of a He-flow microcryostat interposing either an indium foil (device A) or thermal grease (device B). The midinfrared optical performance and electrical characteristics of the devices have been reported elsewhere.[7] The microprobe apparatus used for Raman and PL measurements is described in detail in Ref. 5. The 476.2 nm line of a Kr^+ laser was focused to a 1 μm spot onto the laser front facet using an incident power density $<10^4$ W/cm^2. AS/S Raman spectra were simultaneously recorded using a notch filter to suppress the Rayleigh scattering.

Moderate strain fields ($<10^{-3}$) are typically present in microelectronic devices due to the deposition of dielectric or metallic thin films and the existence of trenches.[8] To determine the strain profile, we measured the PL spectra along device B front facets while it was not in operation. Figure 1 maps the shift ΔE of the PL peak in the GaAs upper cladding layer with respect to the direct exciton energy transition at room temperature (1.4216 eV at 296 K). Values $\Delta E>0$ ($\Delta E<0$) correspond to compressive (tensile) stress. The regions far from the laser ridge and the device ends (80 μm $<|Y|<140$ μm) are unstressed. The tensile strain in the central part of the ridge ($|Y|<13$ μm) and the compressive strain at the edges arise from the surface discontinuity. Abrupt stress variations around the edges are typical of ridge waveguides.[9] The presence of a biaxial stress on GaAs epilayers splits the heavy-hole (HH) and light-hole (LH) excitons and shifts their energy levels linearly with the in-plane strain $\delta_{\|}=\Delta a_{\|}/a$. This splitting is too small to be resolved in our case, due to the relatively broad PL linewidth ($\sim$10

[a]Electronic mail: spagnolo@fisica.uniba.it
[b]Electronic mail: scamarcio@fisica.uniba.it

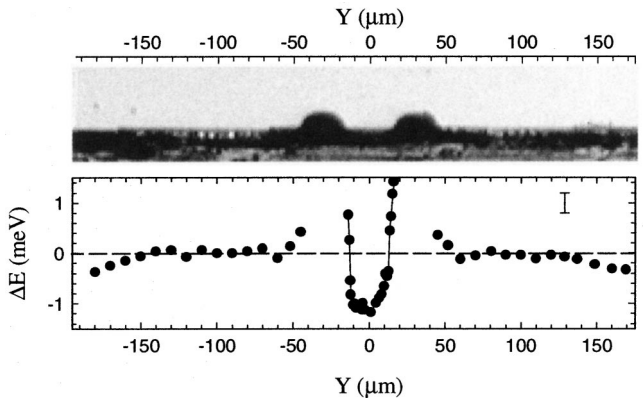

FIG. 1. Typical PL peak energy shift profile measured for the upper cladding layer with device A off. The zero-energy value is indicated for clarity by the dashed line. The origin of the Y axis corresponds to the center of the laser ridge. The picture shows the cross section of device A. The laser front facet extends in the region $-15\ \mu\text{m} < Y < 15\ \mu\text{m}$.

meV) at 140 K, and therefore, we ascribe the observed PL band to a superposition of HH and LH excitonic transitions. Accordingly, the measured maximum value $|\Delta E| \sim 1.5$ meV, gives an upper limit for the in-plane strain $|\delta_{\|}| < 3\times10^{-4}$.[10] A similar PL peak profile is found in the lower cladding layer, although the maximum ΔE value is ~50% lower. Analogous results were obtained for device A. This technique cannot be used for the active region since the related PL spectra appear as a superposition of at least three different transitions between quantized states, difficult to separate unambiguously.

The application of a biaxial stress splits the three-fold degenerate longitudinal optical (LO) and transverse optical (TO) phonons into doublet and singlet modes.[11] We used a backscattering geometry with the incoming and collected scattered light both propagating along the (110) crystal axis. Raman selection rules allow the observation of the TO_D doublet only.[11] For GaAs, the relation between the TO_D energy shift and $\delta_{\|}$ is:[12]

$$\frac{\Delta\omega_{TO_D}}{\delta_{\|}} = -0.34\times10^{3}\ \text{cm}^{-1}. \quad (1)$$

To separate the strain and temperature effects, we measured the Raman spectra in a stress-free region of the upper cladding layer ($Y \sim 100\ \mu$m) with the device off and extracted two calibration curves: The TO phonon energy and the related AS/S intensity ratio, as a function of the temperature, in the range of 50 K–300 K. The local lattice temperature T_L with the device on was extracted from the AS/S intensity ratio. A comparison between the measured TO_D phonon energy and the unstressed value at T_L gives the local lattice strain. Note that we cannot use our approach to determine the temperature and strain in the active regions due to the presence of hot-phonon effects, which may lead to an overestimate of the lattice temperature if using the AS/S ratio calibration curve.[13]

Besides the central part of the ridge ($Y=0$), we focused our attention on the edges ($Y=\pm15\ \mu$m in Fig. 1), where calculations predict the strongest thermally induced strain.[3] Figure 2 shows the local lattice temperature and strain measured in the upper cladding layer as a function of the electrical power density at the heat sink temperature $T_H = 140$ K. T_L increases at a rate of 5.7 K cm^2/kW and 4.2 K cm^2/kW, for devices A [Fig. 2(a)] and B [Fig. 2(b)], respectively. The lower rate for device B indicates that a measurable contribution to the total thermal resistance of the device originates from the mounting. This contribution is reduced when using a thermal grease, instead of an In foil, to improve the thermal contact between the device and the heat sink.[14]

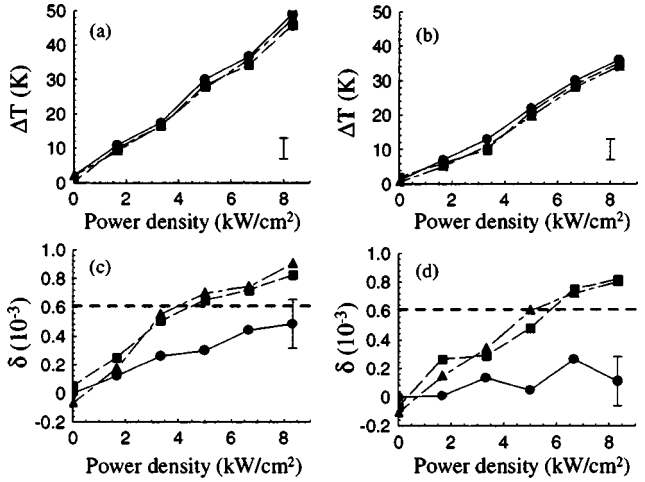

FIG. 2. Lattice temperature (a, b) and misfit strain (c, d) measured in the upper cladding layer as a function of the electrical power density for devices A (a, c) and B (b, d). (●) Center of the laser ridge ($Y=0$); (■) right-hand side edge of the laser ridge ($Y=+15\ \mu$m); (▼) left-hand side edge of the laser ridge ($Y=-15\ \mu$m). The dashed lines in panels (c) and (d) mark the critical strain value before relaxation for a 4.5 μm thick GaAs epilayer.

Figures 2(c) and 2(d) show that increasing electrical power causes tensile strain in the cladding layer. The largest strain develops at the edges of the laser ridge and increases with electrical power at a rate of $\sim1.05\times10^{-4}$ cm^2/kW and 1.0×10^{-4} cm^2/kW for devices A [Fig. 2(c)] and B [Fig. 2(d)], respectively, while the strain in the center of the ridge either increases with a 50% lower rate [see Fig. 2(c)] or remains almost negligible [see Fig. 2(d)]. Figures 2(c) and 2(d) show the calculated onsets for strain relaxation in a 4.5 μm thick GaAs epilayer, using the excess stress model.[15] At power densities larger than ~5 kW/cm^2, the strain at the edges of the ridge exceeds the critical value ($\delta_C = 0.61\times10^{-3}$) for the generation of misfit dislocations and the propagation of lattice defects, leading to lattice deterioration. In fact, we observe device failure at 10 kW/cm^2 (device A) and 12 kW/cm^2 (device B).

Figure 3 shows the calculated temperature and shear stress contours on the laser front facet obtained from a two-dimensional model of thermal transport and thermally induced stress.[16] The lower shear stress values reported in Ref. 3 are mainly due to the different device structures exploiting buried stripes, which greatly reduce the total amount of shear stress that builds up during operation. However, in both cases, the maximum shear stress builds up at the edges of the ridge waveguide in the active and cladding layers.

Comparing Raman spectra measured before and after the device failure confirms that the starting points for device failure are the edges of the laser ridge where the crystal lattice suffers the largest strain field. Figure 4 shows the spectra taken at the right-hand side edge of the device A facet

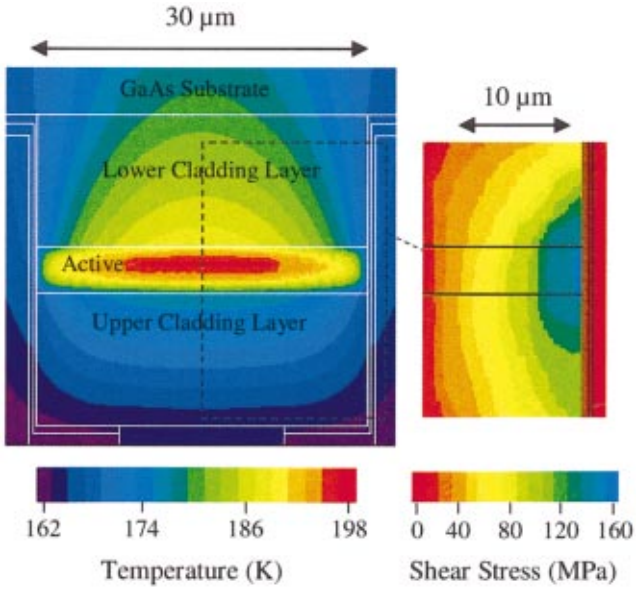

FIG. 3. (Color) Computed temperature and shear stress contours in the ridge region of the QCL. The solid lines display the geometry of the different materials used in the simulation. The shear stress contours is symmetric with respect to the $Y=0$ axis and is shown for the region delineated by the dashed line. The simulation includes also the Au contact layer, the solder, and the laser heat sink.

in both claddings and in the active region. Before device failure (dashed curves in Fig. 4) the Raman spectra coincide with those measured in crystalline GaAs. After device failure (solid curve in Fig. 4) ''forbidden'' LO modes appear in Figs. 4(b) and 4(c). This is ascribed to the relaxation of the scattering selection rules due to lattice structural disorder. The lower cladding layer retains its crystal quality since no significant modification appears in the spectrum taken after device failure. This trend has been observed for all of the Raman spectra taken at the edges of the ridge in both devices. Whereas, the spectra measured in the center of the ridge

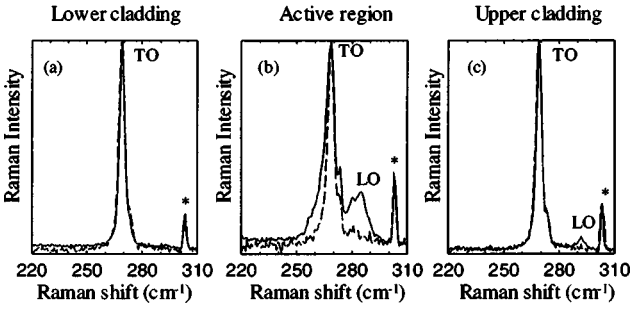

FIG. 4. Raman spectra taken from the right-hand side edge of the ridge ($Y=+15$ μm) of device A in the two claddings (a, c) and the active region (b), before (dashed curve) and after (solid curve) device failure. The appearance of the LO phonon band in the spectra taken after device failure is due to lattice structural disorder and a partial relaxation of scattering selection rules. The (*) symbol marks a plasma line of the Kr^+ laser.

show no crystal deterioration in the cladding layers and only a barely visible LO phonon mode in the active region after the device failure.

In conclusion, our results show that during operation of ridge-waveguide QCLs mounted epilayer down to the heat sink, a thermally induced tensile strain field builds up. At power densities larger than ~ 5 kW/cm^2, the strain overtakes the critical value for the generation of misfit dislocation, causing plastic relaxation in the cladding and active layers and eventually leading to device failure. A substantial improvement in the thermoelastic performance may be obtained using weakly index guided QCL cavities with shallow trenches and proton implanted GaAs channels for lateral current confinement.

This work was partly supported by INFM and MURST, cluster 26 ''Materiali Innovativi,'' project No. P5WP2, FIRB project No. RBAU01E8SS, and by the European Union via the SUPERSMILE Project IST-1999-14193.

[1] C. Gmachl, F. Capasso, D. L. Sivco, and A. Y. Cho, Rep. Prog. Phys. **64**, 1533 (2001).
[2] C. Sirtori, H. Page, and C. Becker, Philos. Trans. R. Soc. London, Ser. A **359**, 505 (2001).
[3] M. Beck, D. Hofstetter, T. Aellen, J. Faist, U. Oesterle, M. Ilegems, E. Gini, and H. Melchior, Science **295**, 301 (2002).
[4] V. Spagnolo, M. Troccoli, G. Scamarcio, C. Becker, G. Glastre, and C. Sirtori, Appl. Phys. Lett. **78**, 1177 (2001).
[5] V. Spagnolo, M. Troccoli, G. Scamarcio, C. Gmachl, F. Capasso, A. Tredicucci, A. M. Sergent, A. L. Hutchinson, D. L. Sivco, and A. Y. Cho, Appl. Phys. Lett. **78**, 2095 (2001).
[6] S. M. Hu, J. Appl. Phys. **70**, R53 (1991).
[7] H. Page, C. Becker, A. Robertson, G. Glastre, V. Ortiz, and C. Sirtori, Appl. Phys. Lett. **78**, 3259 (2001).
[8] I. De Wolf, Semicond. Sci. Technol. **11**, 139 (1996).
[9] C. Corvasce, V. Spagnolo, G. Scamarcio, M. Lugarà, F. Adduci, M. Ferrara, M. Sibilano, S. Pellegrino, M. Del Giudice, and M. G. Re, Proc. SPIE **2648**, 360 (1995).
[10] In GaAs, the HH and LH excitonic energies shift with the strain according to the following relations: $E_{HH}=\delta_{\|}\times 4.55$ and $E_{LH}=\delta_{\|}\times 11.23$, [see, e.g., S. Logothetidis, M. Cardona, L. Tapfer, and E. Bauser, J. Appl. Phys. **66**, 2108 (1989)]. The upper limit for strain is obtained using the HH relation.
[11] F. Cerdeira, C. J. Buchenauer, F. H. Pollak, and M. Cardona, Phys. Rev. B **5**, 580 (1972).
[12] G. Landa, R. Carles, C. Fontane, E. Bedel, and A. Munoz-Tague, J. Appl. Phys. **66**, 196 (1989).
[13] V. Spagnolo, G. Scamarcio, M. Troccoli, F. Capasso, C. Gmachl, A. M. Sergent, A. L. Hutchinson, D. L. Sivco, and A. Y. Cho, Appl. Phys. Lett. **80**, 4303 (2002).
[14] The contribution to the total thermal resistance of the device due to the mounting may be extracted driving the device in pulsed mode, using pulse widths <1 μs and low repetition rates to avoid excess thermal energy transfer from the semiconductor chip to the heat sink and thus prevent self-heating effects. [See V. Spagnolo, M. Troccoli, G. Scamarcio, C. Becker, G. Glastre, and C. Sirtori, Appl. Phys. Lett. **78**, 1177 (2001)].
[15] J. Y. Tsao, B. W. Dodson, S. T. Picraux, and D. M. Cornelison, Phys. Rev. Lett. **59**, 2455 (1987).
[16] The simulation of the thermoelastic behavior of the device was done with a commercial finite-element software package (FLEXPDE). An electrical power density of 8.3 kW/cm^2 and temperature dependent thermal conductivities were used. The semiconductor elastic properties were approximated using isotropic elastic constants, the Young's modulus $E=86$ GPa and the Poisson's ratio $n=0.31$.